ACTA PHYSIOLOGICA

Inhibiting Pyruvate Kinase Muscle Isoform 2 Regresses Group 2 Pulmonary Hypertension Induced by Supra-coronary Aortic Banding

Journal:	*Acta Physiologica*
Manuscript ID	APH-2021-03-0174.R3
Manuscript Type:	Regular Paper
Date Submitted by the Author:	12-Oct-2021
Complete List of Authors:	Xiong, Ping ; Queen's University, Medicine Motamed, Mehras; Queen's University, Medicine Chen, Kuang-Hueih; Queen's University, Medicine Dasgupta, Asish; Queen's University, Medicine Potus, Francois; Queen's University, Medicine Tian, Lian; University of Strathclyde, Strathclyde Institute of Pharmacy and Biomedical Sciences Martin, Ashley; Queen's University, Medicine Mewburn, Jeffrey; Queen's University, Medicine Jones, Oliver; Queen's University, Medicine Thébaud, Arthur; Queen's University, Medicine Archer, Stephen; Queen's University, Medicine
Key Words:	Uncoupled glycolysis, right ventricular hypertrophy, Aortic stenosis, Heart failure with preserved ejection fraction, Shikonin, pyruvate kinase muscle isoform 2

Inhibiting Pyruvate Kinase Muscle Isoform 2 Regresses Group 2 Pulmonary Hypertension Induced by Supra-coronary Aortic Banding

Ping Yu Xiong[1,2], Mehras Motamed[1], Kuang-Hueih Chen[1], Asish Dasgupta[1], François Potus[1], Lian Tian[1], Ashley Martin[1], Jeffrey Mewburn[1], Oliver Jones[1], Arthur Thébaud[1], and Stephen L. Archer[1,3]

[1]Department of Medicine, Queen's University, Kingston, ON, Canada.

[2]Department of Biomedical and Molecular Sciences, Queen's University, Kingston, ON, Canada.

[3]Queen's Cardiopulmonary Unit (QCPU), Kingston, ON, Canada

Stephen L. Archer MD, FRCP(C), FAHA, FACC

Professor, Head Department of Medicine, Queen's University

Director Queen's Cardiopulmonary Unit

Program Medical Director KGH, HDH, SMOL

Etherington Hall, Room 3041

94 Stuart St., Kingston, Ontario, Canada, K7L 3N6

Preferred E-mail: stephen.archer@queensu.ca

Keywords: Uncoupled glycolysis; left ventricular hypertrophy; right ventricular hypertrophy aortic stenosis; heart failure with preserved ejection fraction (HFpEF); shikonin; pyruvate kinase muscle isoform 2 (PKM2);

Abstract Word count 250

Introduction: Group 2 pulmonary hypertension (PH) has no approved PH-targeted therapy. Metabolic remodeling, specifically a biventricular increase in pyruvate kinase muscle (PKM) isozyme 2 to 1 ratio, occurs in rats with Group 2 PH induced by supra-coronary aortic banding (SAB). We hypothesize that increased PKM2/PKM1 is maladaptive and inhibiting PKM2 would improve right ventricular (RV) function.

Methods: Male, Sprague-Dawley SAB rats were confirmed to have PH by echocardiography and then randomized to treatment with a PKM2 inhibitor (intraperitoneal shikonin, 2 mg/kg/day) vs. 5% DMSO (n=5/group) or small interfering RNA targeting PKM2 (siPKM2) vs. siRNA controls (n=7/group) by airway nebulization.

Results: Shikonin-treated SAB rats had milder PH (PAAT 32.1±1.3 vs. 22.1±1.2 ms, p=0.0009) and lower RV systolic pressure (RVSP) (31.5±0.9 vs. 55.7±1.9 mmHg, p<0.0001) versus DMSO-SAB rats. siPKM2 nebulization reduced PKM2 expression in the RV, decreased PAAT (31.7±0.7 vs. 28.0±1.3 ms, *p*=0.025), lowered RVSP (30.6±2.6 vs. 42.0±4.0 mmHg, *p*=0.032), and reduced diastolic RVFW thickness (0.69±0.04 vs. 0.85±0.06 mm, *p*=0.046). Both Shikonin and siPKM2 regressed PH-induced medial hypertrophy of small pulmonary arteries.

Conclusion: Increases in PKM2/PKM1 in the RV contributes to RV dysfunction in Group 2 PH. Chemical or molecular inhibition of PKM2 restores the normal PKM2/PKM1 ratio, reduces PH, RVSP and RVH, and regresses adverse PA remodeling. PKM2 merits consideration as a therapeutic cardiac target for Group 2PH.

Introduction

Group 2 pulmonary hypertension (PH) is due to left heart disease and is the most prevalent type of PH.[1] It often occurs as a complication of systemic arterial hypertension, diastolic dysfunction of the left ventricle, or valvular heart diseases, such as aortic stenosis or mitral valve disease. Group 2 PH is defined by a resting mean pulmonary artery pressure >20 mmHg and elevated left heart filling pressure (pulmonary capillary wedge pressure >15 mmHg).[2] Group 2 PH often results in heart failure (HF). Group 2 PH is present in 47% of patients with HF with reduced ejection fraction (HFrEF)[3], and 69% in patients with HF with preserved ejection fraction (HFpEF)[4]. In a population based epidemiologic study, Group 2 PH was 10-fold more prevalent than group 1 PH and conferred a 7.2-fold increase in standardized mortality rates[5]. In 2012-2013, 669,600 (3.5%) Canadians were living with HF[6], increased 30% from 467,700 in 2000-2001[6]. With aging of the population, the prevalence of HF will continue to rise, and the prevalence of group 2 PH is expected to rise accordingly. There are no approved PH-targeted medications for group 2 PH and developing therapies could have major public health benefit.

To develop effective therapies, the pathophysiology and underlying molecular mechanisms of group 2 PH development must be better understood. Preclinical models are helpful to identify the molecular pathways that promote the two major characteristics of group 2 PH, namely obstructive pulmonary vascular remodeling and RVF. Previously, we discovered a marked biventricular upregulation of pyruvate kinase muscle isozyme 2 (PKM2) relative to PKM1 expression in the supra-coronary aortic banding (SAB) rat model of group 2 PH.[7] Pyruvate kinase catalyzes the final, rate-limiting step of glycolysis, producing pyruvate which enters the mitochondria and fuels Krebs cycle. PK exists in two isoforms: PKM2 and PKM1. PKM2 has lower activity than PKM1. Increased PKM2 expression reduces the conversion of

phosphoenolpyruvate to pyruvate, thereby favoring uncoupled cytosolic glycolysis over glucose oxidation. An increased PKM2/PKM1 ratio also increases NADPH production and cellular hypertrophy.[7] Although the observed increase in PKM2/PKM1 ratio is predicted to favor uncoupled glycolysis over glucose oxidation, as it does in pulmonary vascular cells of Group 1 PH[8, 9], we do not know whether this ventricular increase in PKM2/PKM1 ratio is adaptive or maladaptive in Group 2 PH. Recently we noted a marked increase of PKM2/PKM1 ratio in the RV of a Group 1 PH model, induced by monocrotaline)[10]. In the monocrotaline RV, improving RV perfusion (achieved by increasing right coronary artery perfusion pressure) normalized the PKM2/PKM1 ratio and improved RV function, suggesting that an increased PKM2/PKM1 ratio is likely maladaptive.

In this study we used SAB to create a robust model of Group 2 PH with evidence of adverse pulmonary vascular remodeling and RVF. To create the SAB model we surgically narrowed the ascending aorta using a clip, thereby mimicking aortic stenosis and causing left ventricle (LV) pressure and volume overload.[7] As the left ventricle hypertrophies (LVH), the left ventricular end diastolic pressure (LVEDP) rises, which then elevates the pulmonary capillary wedge pressure (PCWP) and engenders group 2 PH.[7] As the disease advances, adverse pulmonary vascular remodeling and RVH ultimately lead to RV dysfunction and failure. We tested the hypothesis that inhibition of PKM2 and/or normalization of the PKM2/PKM1 ratio would be beneficial in the SAB model. To inhibit PKM2 we used intraperitoneally (IP) administered shikonin, a lipid soluble, naphthoquinone that is a Chinese herbal remedy derived from root epidermal cells of *Lithospermum erythrorhizon*[11]. In a separate SAB cohort, small interfering RNA targeting PKM2 (siPKM2), which was validated for efficacy, modified for use in vivo, and delivered by airway nebulization, was used to treat SAB PH. Chemical or molecular inhibition of PKM2

normalized the RV's PKM2/PKM1 ratio, improved RV function and regressed pulmonary vascular disease. Thus, the biventricular increase in PKM2/PKM1 is maladaptive and correcting this abnormality has therapeutic benefit.

Results

SAB surgery produced moderate to severe PH. There was no significant difference between control and treatment groups before the initiation of shikonin or siPKM2 therapy (Figure 2A, C, E, G, I, K). Echocardiography comparing SAB DMSO vs. Sham DMSO showed an increase of systolic and diastolic LVFW thickness (systole: 4.12±0.14 vs. 3.47±0.20 mm, p=0.03; diastole: 2.76±0.13 vs. 2.18±0.26 mm, p=0.06) (Figure 2F & H) and systolic and diastolic RVFW thickness (systole: 1.43±0.04 vs. 1.23±0.07 mmHg, p=0.04; diastole: 1.10±0.07 vs. 0.75±0.12 mmHg, p=0.03) (Figure 2J & L). Consistent with the development of PH and a reduction in RV function in the SAB model, PAAT was significantly shorter in the SAB vs. sham group (22.10±1.24 vs. 34.69±1.18 ms, p=0.0005), and TAPSE was reduced (2.12±0.15 vs. 3.16±0.17 mm, p=0.005) (Figure 2 B & D). Similar to the SAB DMSO group, the SAB siControl rats achieved similar level of TAPSE reduction, increase in LVFW systolic and diastolic thickness, and increase in RVFW systolic thickness. Despite similar protocols, the severity of group 2 PH intervention was less in this siRNA cohort of rats versus the initial shikonin cohort. For example, the SAB siControl group had significantly higher PAAT (28.02±1.26 vs. 22.10±1.24 mm, p=0.009) and lower diastolic RVFWT (0.85±0.06 vs. 1.10±0.07 mm, p=0.02) compared the SAB DMSO group (Figure D & L).

After 2 weeks treatment with shikonin or siPKM2, PAAT was significantly prolonged, reflecting a reduction in PH. In the SAB shikonin vs. SAB DMSO group PAAT also increased (32.1±1.3 vs. 22.1±1.2 ms, p=0.0009). Likewise, PAAT increased in the SAB siPKM2 vs. SAB siControl group (31.7±0.7 vs. 28.0±1.3 ms, p=0.025) (Figure 2D). TAPSE did not improve in SAB shikonin versus SAB DMSO group. In contrast, siPKM2 treatment significantly improved TAPSE (2.42±0.06 vs. 1.99±0.13 mm, p=0.009) compared to SAB siControl. Although neither shikonin

nor siPKM2 treatment reduced LVFW thickness, both treatments reduced RVFW thickness relative to their respective controls (Figure 2F, H, J, L).

Left heart catheterization showed significantly elevated LVSP in the SAB DMSO vs. Sham DMSO group (237.7±1.7 vs. 85.6±3.7 mmHg, $p<0.0001$). Consistent with the reproducibility of the surgical technique for SAB in both cohorts, there was no significant difference between the LVSP of SAB DMSO vs. SAB siControl group (Figure 3A). However, right heart catheterization showed a significant decrease in RVSP in SAB shikonin vs. SAB DMSO rats (31.5±0.9 vs. 55.7±1.9 mmHg, $p<0.0001$) (Figure 3C). Similarly, there was also a significant decrease of RVSP in SAB siPKM2 vs. SAB siControl group (30.6±2.6 vs. 42.0±4.0 mmHg, $p=0.032$). Pulmonary vascular resistance (PVR) was significantly reduced in SAB shikonin vs. SAB DMSO group (0.06±0.01 vs. 0.31±0.03 mmHg/(mL/min), $p=0.004$) (Supplementary Figure 1B). In contrast, there was no difference between PVR of SAB siPKM2 vs. SAB siControl (Figure 1B). Cardiac output (CO) did not improve with shikonin or siPKM2 treatment relative to their respective controls (Supplementary Figure 1A). There was a trend toward lower LVEDP in SAB shikonin vs. SAB DMSO group (25.9±1.9 vs. 33.7±2.3 mmHg, $p=0.08$) and SAB siPKM2 vs. SAB siControl (22.5±2.5 vs. 29.0±2.2 mmHg, $p=0.08$) (Figure 3B).

Shikonin treatment caused slight but marked weight reduction in both the sham and SAB rats. However, the weight stabilized after 1 week of daily shikonin 2 mg/kg IP treatment (Supplementary Figure 2). Both shikonin and siPKM2 treatment of SAB rats reduced RV myocyte cross-sectional area vs. their respective controls (473±124 vs. 1145±315 μm^2, $p<0.0001$; 286±117 vs. 520±199 μm^2, $p<0.0001$) (Figure 4). Moreover, there was significant reduction in RV weight and RV/body weight ratio in shikonin treated SAB rats compared to DMSO treated rats (Supplementary Figure 3B, E). The weight loss caused by shikonin did not significantly alter the

effective of the banding, as demonstrated by similar systolic and diastolic blood pressure proximal to the band (Supplementary Figure 3F, G). Likewise, both shikonin and siPKM2 treatment of SAB rats reduced the percent pulmonary vascular wall thickness compared to their respective controls (18.7±2.2 vs. 47.2±4.3 %, p<0.0001; 24.0±1.4 vs. 38.5±4.5%, p=0.007) (Figure 5).

In the RV of SAB shikonin vs. SAB DMSO group Western blot showed a significant downregulation of PKM2 (0.31±0.04 vs. 0.78±0.05, p <0.0001) and an increase in the PKM2/PKM1 ratio (0.37±0.05 vs. 1.47±0.14, p <0.0001) (Figure 6A, C, and E). There was a parallel trend toward PKM1 upregulation in SAB shikonin vs. SAB DMSO group (0.87±0.07 vs. 0.57±0.09, p =0.07) (Figure 6D). Treatment with siPKM2 also decreased the PKM2/PKM1 ratio (1.0±0.22 vs. 0.70±0.17, p=0.009) (Figure 6B & H); however, while the ratio changed significantly, the individual changes in PKM2 and PKM1 expression did not achieve statistical significance (Figure 6F & G). SAB increased the PKM2/PKM1 ratio in the LV and was significantly reduced by shikonin (Supplementary Figure 5).

Immunofluorescent imaging of the lung cross-section showed that there was a trend towards PKM1 reduction in the siPKM2 treated rats vs. siControl (3549±1720 vs. 7779±1857 fluorescent units/μm^2, p=0.059) (Figure 7E). There was no difference between the PKM1 expression in the small pulmonary artery of siPKM2 treated rats vs siControl rats (Figure 7J). The expression of PKM2 in SAB rats was significantly reduced in siPKM2 treated SAB rats compared to SAB rats nebulized with siControl (1893±923 vs. 6612±1951 fluorescent units/μm^2, p=0.035) (Figure 8E). Similarly, there was no difference between the PKM2 expression in the small pulmonary artery of siPKM2 treated rats vs siControl rats (Figure 8J), suggesting the pulmonary vasculature was not targeted by our nebulized siPKM2 therapy. Supplementary figure 7 illustrates how the PKM fluorescence from small pulmonary arteries was measured.

Discussion

This study reveals a metabolic basis for the adverse functional and structural remodelling in the right ventricle and pulmonary vasculature in an experimental Group 2 PH model that mimics aortic stenosis. First, we confirmed our prior findings that the PKM2/PKM1 isoform profile of pyruvate kinase, the terminal enzyme in glycolysis, is shifted in the RV in group 2 PH. This shift (an increase in PKM2 over PKM1) occurs in both the RV and LV and would be predicted to favour uncoupled aerobic glycolysis[12]. Second, we show for the first time that correction of the elevated PKM2/PKM1 ratio, whether achieved chemically (shikonin) or by a molecular intervention (siPKM2) improves RV function while reducing RVH and simultaneously regressing adverse pulmonary vascular remodeling. This is associated with a trend for reduction in LVEDP with both therapies ($p=0.08$). A strength of this study is the observed concordant benefits of chemical and molecular strategies to inhibit PKM2 (shikonin and siPKM2, respectively). In addition, we employed a regression strategy to test our therapies, ensuring that as in human diseases causing Group 2 PH, like aortic stenosis, the ventricular hypertrophy and PH were established in our rat model before therapy was initiated. Also relevant to human disease the therapy was utilized without eliminating the cause of the Group 2 PH (i.e. the banding remained in place). The features of experimental design makes our preclinical findings more relevant to the human condition. In aggregate these data demonstrate that the biventricular increase in PKM2/PKM1 is a maladaptive feature of Group 2 PH and shows that correction of this metabolic abnormality has therapeutic benefit, even when the cause of the Group 2 PH (the SAB) remains in place. A final strength of this study is the long history of human consumption of shikonin[13], an ancient Chinese herbal remedy, which suggests moving this drug into a clinical trial in humans would be feasible.

Altered RV metabolism, characterized by increased uncoupled glycolysis and decreased glucose oxidation, has been observed in a pulmonary arterial banding (PAB)-induced RVH rat model and in Group 1 PH [the monocrotaline (MCT) rat model of pulmonary arterial hypertension (PAH), and humans with PAH][14]. On a molecular level, increased glycolysis and decreased glucose oxidation can be mediated by several mechanisms. One mechanism that increases uncoupled glycolysis is activation of pyruvate dehydrogenase kinases (PDKs), enzymes which phosphorylate and inhibit pyruvate dehydrogenase (PDH)[15]. Fang et al. demonstrated that in PAB rat model of RVH, there was also increased maladaptive increases in fatty acid oxidation (FAO), which suppressed glucose oxidation[14]. Inhibiting FAO in this model led to increased glucose oxidation and enhancement of RV function, via activation of the Randle cycle[16].

While the cardiac effects of PKM2 are unknown, Zhang et al.[8] and Caruso et al.[9] discovered a similar increase in PKM2/PKM1 ratio in the pulmonary vascular fibroblasts and endothelial cells, respectively in both Group 1 PH animal models and PH patients. Moreover, Zhang et al. also used shikonin in their study and demonstrated that shikonin reversed the glycolytic state of PH-fibroblasts, which decreased cell proliferation[8]. Thus, in Group 1 PH (also known as pulmonary arterial hypertension) the increased PKM2/PKM1 ratio is maladaptive and contributes to disease progression. Since it can be difficult to clinically differentiate amongst PH groups, beneficial effects of correcting the PKM2/PKM1 ratio in several forms of PH is reassuring were this therapy to move to clinical trials in patients.

Shikonin-treated SAB rats have reduced PH (evident as lower RVSP and PVR), as determined by high-fidelity hemodynamics. They also had a reduction in RVH and a regression of pulmonary arterial muscularization on histological analysis. Since Group 2 PH is a disease affecting the entire cardiopulmonary system, the finding that PKM2-targeted therapies benefit both

the heart and lung is a desirable attribute for a therapy with the potential for use in humans. The beneficial effects of therapy were associated with a significant reduction in the PKM2/PKM1 ratio in the SAB RV, relative to DMSO treated animals. In addition, the LVEDP of shikonin-treated SAB rats also showed a strong trend towards reduction compared to DMSO-treated SAB rats (Figure 3B). This is consistent with the observation that the PKM2/PKM1 ratio is increased in both ventricles and that the function of both ventricles is improved toward normal by shikonin therapy (Figure 6A and Supplementary Figure 5).

However, we acknowledge that shikonin may have effects that are unrelated to PKM2 inhibition. For instance, Kim et al. noted that shikonin can upregulate receptor-interacting serine/threonine-protein 1 (RIP1)[17]. Chen et al. showed that shikonin inhibits chemokine receptor 5 (CCR5)[18]. Because of the off-target effects of shikonin, we can only conclude that there is an association between shikonin-induced PKM2 down-regulation in SAB rats and the observed shikonin-induced improvement in RV function. Moreover, the observed upregulation of PKM1 in shikonin-treated SAB rats was unexpected. Had we only used shikonin it would have been unclear whether the upregulation of PKM1 was directly related to shikonin or occurred indirectly via other molecular mechanisms.

To address the concerns about molecular mechanisms of action, we tested the efficacy of a validated siPKM2 in SAB rats (Supplementary Figure 4), which we delivered by airway nebulization, once Group 2 PH and RVH were established. SAB rats nebulized with siPKM2 also had improved RV function (increased TAPSE), less severe RVH (reduced diastolic RVFW thickness) and less severe PH (reduced PAAT), compared to SAB rats receiving siControl (Figure 2). High fidelity cardiac catheterization confirmed these echocardiographic measurements, showing a significant reduction in RVSP in the siPKM2 group (Figure 3). As with shikonin

therapy, siPKM2, reduced PKM2/PKM1 ratio (Figure 6B); however, unlike shikonin this molecular therapy did not significantly elevate PKM1 expression. The concordant results demonstrate that inhibiting the PKM2 is an effective therapeutic strategy for treating group 2 PH and puts the emphasis for the benefit on PKM2 reduction, rather than changes in PKM1 expression.

Limitations: When tested *in vitro* in pulmonary artery smooth muscle cells isolated from monocrotaline rat made in our lab, siPKM2 down regulates both PKM2 and PKM1. Initially, we are also puzzled by this finding. Given that PKM2 and PKM1 are splice variants and are transcribed from the same gene, there is a time when they co-exist on one mRNA after transcription before the splicing take place, we suspect that *in vitro* experiment with siPKM2 bind to the pre-spliced mRNA and resulted in knock down of both PKM2 and PKM1 in equal proportion. However, in vivo the predominant effect of siPKM2 was on the PKM2 isoform.

The beneficial effect of both therapies on adverse pulmonary remodeling was significant. In the case of shikonin this may reflect a direct action on the small pulmonary arteries. However, siPKM2 did not lower either PKM1 or PKM2 in the small pulmonary arteries. These findings indicate that the benefit to the pulmonary arteries was secondary, occurring not because of siPKM2 targeting the resistance pulmonary arteries but indirectly, as a result of improvement in the LV function and tending to reduce LVEDP, which is the driver of group 2 PH (Figure 7 & 8)

Future Directions: Shimauchi et al. showed that PKM2/PKM1 is also increased in patients with both compensated and decompensated RV hypertrophy[19], which is consistent with our observations in a rat model of group 2 PH. In their study, Shimauchi et al. observed sustained activation of Poly ADP-ribose polymerase 1 (PARD1), which helped to enhance PKM2 nuclear translocation and mediate the resulting Warburg effect[19]. In light of the long history of human use of shikonin, albeit not validated by a conventional randomized clinical trial (RCT), the concordant

effects of shikonin and siPKM2 in experimental group 2 PH would, if replicated by others, support further testing. We suggest that after comprehensive preclinical toxicity and pharmacology studies, there is a rational basis for a phase I clinical trial testing shikonin in healthy volunteer to evaluate safety, optimal route of administration, and dose ranges before testing the drug in patients with Group 2 PH.

Materials and Methods

The experimental protocol has been approved by Queen's University Animal Care Committee and the University Research and Ethics Board (Protocol # 1714). All experiments were conducted following best experimental practices with careful attention to ensuring adequacy of sample size and blinding of investigators to treatment groups, as described[20].

Experimental Design

Five-week-old male Sprague Dawley rats (Strain Code: 400, Charles River, Wilmington, USA) were raised in the Queen's Animal Care Facility. After a week of acclimatization, SAB or sham surgery was performed generating 10 rats in each group. Echocardiography was performed 6 weeks post-surgery to confirm the development of group 2 PH. The SAB and sham groups were then randomly assigned to receive either DMSO or shikonin, creating a total of four cohorts (n=5 each): DMSO-treated SAB, shikonin-treated SAB, DMSO-treated sham, and shikonin-treated sham. Treatments were daily intraperitoneal injections of either shikonin (2 mg/kg dissolved in 5% DMSO by boiling for 3 minutes, Sigma-Aldrich, St. Louis, USA) or 5% DMSO. This dose was based on the literature[17, 18] and preliminary experiments as being effective and non-toxic. Terminal catheterization and tissue harvesting were performed 9-weeks post-surgery (Figure 1A).

To gain molecular certainty whether the therapeutic effects of shikonin were primarily the results of its effects on PKM2 we studied a second male rat cohort that we treated with siPKM2 (n=8) vs. siControl (n=8). The siControl was scrambled RNA. Both siRNAs were delivered in the Invivofectamine 3.0 Reagent (Catalog #: IVF3001, Thermo Fisher Scientific, Waltham, USA). Echocardiography was performed 6 weeks post-surgery to confirm the development of group 2 PH. The SAB rats were randomized into 2 groups to receive either siPKM2 (1 nmol) or siControl

(1 nmol) nebulized into the lung every 3 days times three. Terminal catheterization and tissue harvesting were performed 9 weeks post-surgery (Figure 1B).

The SAB Model

The SAB model is the most commonly used model for preclinical studies of Group 2 PH.[21-23] In this model, a clip or a suture tie is placed around the ascending aorta of 3 to 4 weeks old rats. As the animals grow bigger, the clip around the ascending aorta progressively impedes aortic outflow and results in LV pressure overload, which subsequently results in development of HFpEF and PH. A 2 cm incision of the skin was made between the second and third ribs, then a 1.5 cm incision of the intercostal muscles layer was made between the second and third ribs. The ribs were retracted, and the ascending portion of the aorta visualized. A size small (3x1mm) Weck® Horizon™ titanium clip (Teleflex, Markham, ON) was placed around the ascending aorta with the help of an applicator. The clip produced a reproducible and uniform 50-60% constriction of the ascending aorta. Following placement of the aortic clip, the second and third ribs were approximated with 4-0 Vicryl™ (polyglactin) in an interrupted suture pattern. Simultaneously, the ventilator was paused for about 2-4 seconds in order to re-inflate the lungs. A 23-gauge chest tube attached to a 10 mL syringe was inserted in the chest prior to chest closure. The muscle layers and the skin were opposed with 4-0 Vicryl™ (polyglactin) sutures and 2 to 3 surgical clips were applied over the skin suture. A syringe attached to the chest tube was used to aspirate air form the pleural space and expand the lung and remove any blood. The chest tube was then removed and the suture tightened to close the incision. The rat was recovered on a heating pad (37ºC) by gradually lowering the anesthesia and maintaining ventilator assisted respiration for 3 minutes prior to extubation. After extubation, rats were returned to their cages, positioned on their sides and observed until they were awake and in stable condition. Standard post-operative care was provided

to minimize pain and risk of wound infection. The operative mortality rate measured at 24 hours was less than 5%.

Echocardiography

Cardiovascular imaging was performed using a Vevo® 2100 (FUJIFILM VisualSonics Inc, Toronto, ON) phased-array, color-Doppler ultrasound system with a 37.5 MHz transducer using frame rates up to 1000/s. Serial 2-dimensional, M-mode and pulsed-wave Doppler ultrasound recordings were performed under anesthesia (inhaled, isoflurane, 1.6–2.0%, mixed with humidified medical air delivered via a cone inhaler). Ultrasound studies were performed weekly beginning 1-week post-surgery to measure RV function and structure [tricuspid annular plane systolic excursion (TAPSE) and right ventricular free wall thickness (RVFWT)]. Pulmonary arterial pressure (PAP) was estimated using the pulmonary artery acceleration time (PAAT), which is inversely proportional to mean PAP, as previously described[24].

Echocardiography data were analyzed using the Vevo® 2100 software. TAPSE, right and left ventricular free wall thickness were estimated using the software's ruler tool and the value was expressed in millimeter. PAAT was measured using the pulmonary acceleration time tool and the value was expressed in milliseconds. Results reflect the average of 3 beats.

Cardiac Catheterization

Rats were anesthetized with isoflurane (1.6–2.0%) and placed on a heated pad at 37ºC (PhysioSuite, Kent Scientific Corp. Torrington, CT, US). SBP, LVESP, and LVEDP were measured in closed-chest rats using a 1.9-F rat pressure-volume catheter (Scisense Inc. London, ON), which was introduced retrograde into the LV via the right common carotid artery, as previously described[7]. Subsequently the catheter was removed and advanced via the right jugular vein retrograde into the RV, where RV pressure-volume loops were acquired, allowing

measurement of RVESP and RVEDP. Finally, the rat was euthanized by exsanguination while deeply anesthetized.

Hemodynamic data were analyzed using iWorx LabScribe v3 (iWorx Systems Inc., Dover, NH, USA). Measurements were made by averaging the results from 5-10 cardiac consecutive cycles that had uniform and appropriate waveforms for both the pressure and volume signals using the software's 'PV loops' tool. Relevant hemodynamic data including systolic and diastolic blood pressure distal to the band (dSBP & dDBP), systolic and diastolic blood pressure proximal to the band (pSBP & pDBP), left ventricular end systolic pressure (LVESP) end diastolic pressure (LVEDP), and right ventricular end systolic pressure (RVESP) end diastolic pressure (RVEDP) were extracted from the table generated using the 'PV loops' tool.

Tissue Collection and Histology

Tissues were harvested immediately following euthanasia. The heart was washed and dissected in ice cold phosphate buffered saline (PBS) solution and the RV was separated from the LV plus septum (LV+S) and weighed. The RV and LV+S were cut into 3-4 small pieces, frozen in liquid nitrogen, and stored at -80 °C. Samples of both ventricles were also fixed with formalin for histology. Picrosirius red staining was used to measure fibrosis, as previously described[7]. The lung was processed similarly. The left lower lobe was inflated and fixed with formalin and later stained with hematoxylin and eosin (H&E).

Immunofluorescence Assessment of PKM2 Expression

Lung tissues from siControl (n=7) and siPKM2 SAB (n=8) treated rats were fixed permeabilized and sectioned (20 µm) onto glass slides. Slides were stained with PKM1 (15821-1-AP, Proteintech, Tucson, AZ, USA) or PKM2 antibody (15822-1-AP, Proteintech, Tucson, AZ, USA) and then a secondary antibody was applied at a concentration of 1:400 (Alexa fluor

488, Catalog # 710369, Invitrogen by ThermoFisher Scientific, Waltham, MA, USA). The tissue slices were covered with 25mm round coverslips and mounted with prolong diamond antifade mounting with DAPI (Catalog # D1306, Invitrogen by ThermoFisher Scientific, Waltham, MA, USA). Tissues were imaged on Leica SP8 confocal microscope with white light laser tuned to 491 nm and the fluorescent signal was collected at 510-660nm, using a 63x 1.4 NA oil immersion objective. Five tile scan acquisitions were performed to include 9 tiles with sampling at 0.3-micron steps for 10 z-steps resulting in 0.5mm x 0.5mm x 3um volume for each sample. Analysis was performed using Leica LAS X 3D analysis software (Leica) measuring total volume of signal in the tile scanned merged images.

siPKM2 RNA Design and Validation

The siRNA duplex specific for rat PKM2 mRNA was sense 5'- GUGUGAACUUGGCCA UGAAUU-3'; antisense 5'- UUCAUGGCCAAGUUCACACUU-3' from exon 10. Control-siRNA (ctrl-siRNA) duplex, a sequence having no homology to any known mammalian transcript, was used as a negative control (sense 5'- CGUUAAUCGCGUAUAAUACGCGUAT-3'; antisense 5'- AUACGCGUAUUAUACGCGAUUAACGAC-3'). The primers used for rat PKM2 were sense: 5'-ATTACCAGCGACCCCACAGAA -3', antisense: 5'- ACGGCATCCTTACACA GCACA-3' (Supplementary Figure 4). The PKM2 siRNA duplex was purchased from Dharmacon, (Lafayette, CO, USA). The control siRNA duplex and primers were purchased from Integrated DNA Technology (IDT, Coralville, IA, USA). For validation of in-vitro siRNAs, we used pulmonary artery smooth muscle cell (PASMC) isolated from monocrotaline rats made from our lab. For in vivo studies, the siRNA against PKM2 and the control siRNA were modified for a higher stability and procured from Integrated DNA Technology. Briefly, 1 nmol siPKM2 or control siRNA was mixed with Invivofectamine 3.0 Reagent (Thermo Fisher Scientific) and

administered to the anesthetized rat by nebulization in 50 µL saline with an aerosol nebulizer (MSA-250-R, Penn-Century Inc, Wyndmoor, Pennsylvania, USA).

***In vivo* siRNA treatment in SAB rats**

SD rats 6 weeks post SAB surgery were randomly assigned to the siControl or the siPKM2 group (n=8 /group). Animals were anesthetized (3% inhaled isoflurane) and nebulized (MicroSprayer; IA-1B; Penn-Century Inc, Wyndmoor, Pennsylvania, USA) with 1 nmole of siPKM2 (*in vivo* Predesigned siRNA s144150, Ambion, Burlington, Ontario, CANADA) or control siRNA (in vivo negative control #1; 4457287, Ambion) suspended in Invivofectamine 3.0 Reagent (IVF3001, Invitrogen). Nebulization of siRNA was repeated every 3-4 days for total of 3 nebulizations per rat. Experiments using nebulized animals were conducted 48 hours after the final siRNA treatment.

Immunoblots

Tissues (LV, RV, and lung) were flash frozen and ground into fine powder using a mortar and pestle. Tissue powder lysates were prepared in cell lysis buffer (Cell Signaling Technologies, Beverly MA, USA). For immunoblot analysis, tissue lysates (40–80 µg) were analyzed on 4–12% NuPAGE gels (Life technologies, Carlsbad, CA, USA). The proteins were electrotransferred to a polyvinylidene difluoride (PVDF) membrane (Life technologies, Carlsbad, CA, USA) and detection of specific proteins was carried out with the antibodies indicated below, using the ECL-Plus Western Blotting Detection System (GE Healthcare, Piscataway, NJ, USA). Total Drp1 (611112) antibody was purchased from BD transduction Laboratories (San Jose, Ca, USA). Antibodies for PKM1 (15821-1-AP), and PKM2 (15822-1-AP) were obtained from Proteintech (Tucson, AZ, USA). Vinculin (V9131) was obtained from Sigma-Aldrich (St. Louis, MO, USA) (SAB4502158).

Statistical Analysis

Values are expressed as mean +/- standard error of the mean (SEM). Statistical comparison between DMSO vs. Shikonin or siControl vs. siPKM2 were performed using paired, parametric, two-tailed Student's t-test. *P-values* > 0.05 were expressed as non-significant (ns). If *p-value* is less than 0.05 or very close to 0.05, the exacted *p-value* was shown. Statistical calculations were performed using GraphPad Prism 9 (GraphPad Software, Inc., La Jolla, CA, USA).

References

1. Xiong PY, Jaff Z, D'Arsigny CL, Archer SL and Wijeratne DT. Evaluation of the Impact of an Echocardiographic Diagnosis of Pulmonary Hypertension on Patient Outcomes. *Canadian Journal of Cardiology Open*. 2020;2:328-336.
2. Simonneau G, Montani D, Celermajer DS, Denton CP, Gatzoulis MA, Krowka M, Williams PG and Souza R. Haemodynamic definitions and updated clinical classification of pulmonary hypertension. *Eur Respir J*. 2019;53.
3. Khush KK, Tasissa G, Butler J, McGlothlin D, De Marco T and Investigators E. Effect of pulmonary hypertension on clinical outcomes in advanced heart failure: analysis of the Evaluation Study of Congestive Heart Failure and Pulmonary Artery Catheterization Effectiveness (ESCAPE) database. *Am Heart J*. 2009;157:1026-34.
4. Thenappan T, Shah SJ, Gomberg-Maitland M, Collander B, Vallakati A, Shroff P and Rich S. Clinical characteristics of pulmonary hypertension in patients with heart failure and preserved ejection fraction. *Circ Heart Fail*. 2011;4:257-65.
5. Wijeratne DT, Lajkosz K, Brogly SB, Lougheed MD, Jiang L, Housin A, Barber D, Johnson A, Doliszny KM and Archer SL. Increasing Incidence and Prevalence of World Health Organization Groups 1 to 4 Pulmonary Hypertension-A Population-Based Cohort Study in Ontario, Canada. *Circulation: Cardiovascular Quality and Outcomes*. 2018;11:e003973.
6. Report from the Canadian Chronic Disease Surveillance System: Heart Disease in Canada. 2018:1.
7. Xiong PY, Tian L, Dunham-Snary KJ, Chen K-H, Mewburn JD, Neuber-Hess M, Martin A, Dasgupta A, Potus F and Archer SL. Biventricular Increases in Mitochondrial Fission Mediator (MiD51) and Proglycolytic Pyruvate Kinase (PKM2) Isoform in Experimental Group 2 Pulmonary Hypertension-Novel Mitochondrial Abnormalities. *Frontiers in Cardiovascular Medicine*. 2019;5.
8. Zhang H, Wang D, Li M, Plecita-Hlavata L, D'Alessandro A, Tauber J, Riddle S, Kumar S, Flockton A, McKeon BA, Frid MG, Reisz JA, Caruso P, El Kasmi KC, Jezek P, Morrell NW, Hu CJ and Stenmark KR. Metabolic and Proliferative State of Vascular Adventitial Fibroblasts in Pulmonary Hypertension Is Regulated Through a MicroRNA-124/PTBP1 (Polypyrimidine Tract Binding Protein 1)/Pyruvate Kinase Muscle Axis. *Circulation*. 2017;136:2468-2485.
9. Caruso P, Dunmore BJ, Schlosser K, Schoors S, Dos Santos C, Perez-Iratxeta C, Lavoie JR, Zhang H, Long L, Flockton AR, Frid MG, Upton PD, D'Alessandro A, Hadinnapola C, Kiskin FN, Taha M, Hurst LA, Ormiston ML, Hata A, Stenmark KR, Carmeliet P, Stewart DJ and Morrell NW. Identification of MicroRNA-124 as a Major Regulator of Enhanced Endothelial Cell Glycolysis in Pulmonary Arterial Hypertension via PTBP1 (Polypyrimidine Tract Binding Protein) and Pyruvate Kinase M2. *Circulation*. 2017;136:2451-2467.
10. Tian L, Xiong PY, Alizadeh E, Lima PDA, Potus F, Mewburn J, Martin A, Chen K-H and Archer SL. Supra-coronary aortic banding improves right ventricular function in experimental pulmonary arterial hypertension in rats by increasing systolic right coronary artery perfusion. *Acta Physiologica*. 2020;n/a:e13483.
11. Tatsumi K, Yano M, Kaminade K, Sugiyama A, Sato M, Toyooka K, Aoyama T, Sato F and Yazaki K. Characterization of Shikonin Derivative Secretion in Lithospermum

erythrorhizon Hairy Roots as a Model of Lipid-Soluble Metabolite Secretion from Plants. *Frontiers in Plant Science*. 2016;7.

12. Archer SL. Pyruvate Kinase and Warburg Metabolism in Pulmonary Arterial Hypertension: Uncoupled Glycolysis and the Cancer-Like Phenotype of Pulmonary Arterial Hypertension. *Circulation*. 2017;136:2486-2490.
13. Andújar I, Ríos JL, Giner RM and Recio MC. Pharmacological properties of shikonin - a review of literature since 2002. *Planta Med*. 2013;79:1685-97.
14. Piao L, Marsboom G and Archer SL. Mitochondrial metabolic adaptation in right ventricular hypertrophy and failure. *Journal of Molecular Medicine*. 2010;88:1011-1020.
15. Piao L, Fang YH, Cadete VJ, Wietholt C, Urboniene D, Toth PT, Marsboom G, Zhang HJ, Haber I, Rehman J, Lopaschuk GD and Archer SL. The inhibition of pyruvate dehydrogenase kinase improves impaired cardiac function and electrical remodeling in two models of right ventricular hypertrophy: resuscitating the hibernating right ventricle. *Journal of molecular medicine (Berlin, Germany)*. 2010;88:47-60.
16. Fang YH, Piao L, Hong Z, Toth PT, Marsboom G, Bache-Wiig P, Rehman J and Archer SL. Therapeutic inhibition of fatty acid oxidation in right ventricular hypertrophy: exploiting Randle's cycle. *Journal of molecular medicine (Berlin, Germany)*. 2012;90:31-43.
17. Kim HJ, Hwang KE, Park DS, Oh SH, Jun HY, Yoon KH, Jeong ET, Kim HR and Kim YS. Shikonin-induced necroptosis is enhanced by the inhibition of autophagy in non-small cell lung cancer cells. *J Transl Med*. 2017;15:123.
18. Chen X, Yang L, Zhang N, Turpin JA, Buckheit RW, Osterling C, Oppenheim JJ and Howard OMZ. Shikonin, a Component of Chinese Herbal Medicine, Inhibits Chemokine Receptor Function and Suppresses Human Immunodeficiency Virus Type 1. *Antimicrobial Agents and Chemotherapy*. 2003;47:2810-2816.
19. Shimauchi T, Omura J, Bonnet SB, Paulin R, Provencher S, Boucherat O and Bonnet S. Abstract 12208: Role Of PKM2 and Oxidative DNA Damage in the Pathogenesis of Right Ventricular Failure Associated With Pulmonary Arterial Hypertension. *Circulation*. 2019;140:A12208-A12208.
20. Provencher S, Archer SL, Ramirez FD, Hibbert B, Paulin R, Boucherat O, Lacasse Y and Bonnet S. Standards and Methodological Rigor in Pulmonary Arterial Hypertension Preclinical and Translational Research. *Circ Res*. 2018;122:1021-1032.
21. Breitling S, Krishnan R, M. GN and Michael KW. The Pathophysiology of Pulmonary Hypertension in Left Heart Disease. *American journal of physiology Lung cellular and molecular physiology*. 2015:L924--L941.
22. Wang Q, Guo Y-Z, Zhang Y-T, Xue J-J, Chen Z-C, Cheng S-Y, Ou M-D, Cheng K-L and Zeng W-J. The Effects and Mechanism of Atorvastatin on Pulmonary Hypertension Due to Left Heart Disease. *PLOS ONE*. 2016;11:e0157171-e0157171.
23. Yin J, Marian K, Julia H, Anja S-K, Juergen B, E. HW, Hermann K and M. KW. Sildenafil preserves lung endothelial function and prevents pulmonary vascular remodeling in a rat model of diastolic heart failure. *Circulation: Heart Failure*. 2011;4:198--206.
24. Urboniene D, Haber I, Fang YH, Thenappan T and Archer SL. Validation of high-resolution echocardiography and magnetic resonance imaging vs. high-fidelity catheterization in experimental pulmonary hypertension. *Am J Physiol Lung Cell Mol Physiol*. 2010;299:L401-12.

Figure Legends:

Figure 1. Experimental design for the supra-coronary aortic banding (SAB) study of Group 2 PH A) shikonin therapy protocol and B) silencing PKM2 by nebulization of small inhibitory RNA targeting PKM2 (siPKM2) protocol. SD, Sprague-Dawley; IP, intraperitoneal; DMSO, dimethyl sulfoxide, Neb, nebulization.

Figure 2. Echocardiography results before and after 2-weeks of therapy with shikonin (2mg/kg IP daily) or silencing pyruvate kinase muscle isoform 2 (siPKM2) nebulization treatment (1nM nebulized every 3 days x 3).
Tricuspid annular plane systolic excursion (TAPSE) A) before and B) after 2-week of shikonin and siPKM2 therapy. Shikonin did not affect TAPSE, but siPKM2 significantly improved TAPSE. Pulmonary arterial acceleration time (PAAT) C) before and D) after shikonin and siPKM2 therapy. Both shikonin and siPKM2 treatment markedly improved PAAT. Systolic left ventricular free wall thickness (LVFWT) E) before and F) after shikonin and siPKM2 therapy. Diastolic LVFWT G) before and H) after shikonin and siPKM2 therapy. Shikonin and siPKM2 treatment did not affect both systolic and diastolic LVFWT. Systolic right ventricular free wall thickness (RVFWT) I) before and J) after shikonin and siPKM2 therapy. Diastolic RVFWT K) before and L) after shikonin and siPKM2 therapy. Shikonin and siPKM2 treatment significantly reduced both systolic and diastolic RVFWT.

Figure 3. Hemodynamic studies. Left and right heart catheterization results show significant reduction of right ventricular systolic pressure (RVSP) in the shikonin and silencing pyruvate kinase muscle isoform 2 (siPKM2) treated supra-coronary aortic banding (SAB) rats vs. DMSO and silencing control (siControl) treated SAB rats. After 2-weeks of shikonin (2mg/kg IP daily) or siPKM2 (1 nmol nebulized every 3 days) treatment, A) there was no significant difference in left ventricular systolic pressure (LVSP); B) there was a trend toward reduction in left ventricular end diastolic pressure (LVEDP); C) there was a reduction right ventricular systolic pressure (RVSP); and D) there was no significant difference in right ventricular end diastolic pressure (RVEDP) in both shikonin and siPKM2 treated SAB rats vs. their respective control SAB rats.

Figure 4. Inhibiting pyruvate kinase muscle isoform 2 (PKM2) with either shikonin or siPKM2 reduces right ventricle (RV) myocyte cross-sectional size.
Hematoxylin and eosin stain of lung cross-section showing supra-coronary aortic banding (SAB) caused marked B) increase in RV myocyte cross-sectional area compared to A) sham rats treated with 5% dimethyl sulfoxide (DMSO). There was marked reduction of RV myocyte cross-sectional area in D) shikonin and F) siPKM2 treated supra-coronary aortic banding (SAB) rats compared to their respective controls B) and E). C) shikonin treatment does not affect RV myocyte size in sham rats. G) illustrated the summary statistics.

Figure 5. Inhibiting pyruvate kinase muscle isoform 2 (PKM2) with either shikonin or siPKM2 reduces distal pulmonary arterial muscularization.
Hematoxylin and eosin stain of lung cross-section showing supra-coronary aortic banding (SAB) caused marked B) increase in pulmonary vascular wall thickness (%) compared to A) sham rats treated with 5% dimethyl sulfoxide (DMSO). There was marked reduction of pulmonary vascular wall thickness (%) in D) shikonin and F) siPKM2 treated supra-coronary aortic banding (SAB)

rats compared to their respective controls B) and E). C) shikonin treatment does not affect pulmonary arterial muscularization in sham rats. G) illustrated the summary statistics.

Figure 6. Immunoblot showing reduction of PKM2/PKM1 ratio in shikonin or siPKM2 treated SAB rats compared to SAB rats treated with DMSO and siControl.
A) Representative Western blot showing upregulation of PKM2 and down-regulation of PKM1 in the SAB-DMSO rats, and treatment with shikonin (2 mg IP daily for 2-week) in SAB rat reduced the expression of PKM2/PKM1 ratio. B) Representative Western blot showing nebulization of siPKM2 (1nM) every 3 days for 2-week in SAB rats reduced the expression of PKM2/PKM1 ratio.

Figure 7. Immunofluorescence (IF) of lung stained with PKM1 antibody showing no significant changes in PKM1 expression in the lungs or small PAs of siPKM2 treated animals vs. siControl.
Representative IF images stained with PKM1 antibody of A-D) lung cross-section or F-I) small pulmonary arteries. There is a trend towards PKM1 expression reduction in the E) lung cross-section of siPKM2 treated supra-coronary aortic banding rats (SAB) rats but not in the siControl treated SAB rats. There is no significant difference in PKM1 expression in the J) small pulmonary arteries.

Figure 8. Immunofluorescence (IF) of lung stained with PKM2 antibody showing significant reduction in PKM2 expression in lungs (but not small PAs) of siPKM2-treated animals vs. siControl. Representative IF images stained with PKM2 antibody of A-D) lung section or F-I) small pulmonary arteries. There is significant reduction in PKM2 expression in the E) lung cross-section of siPKM2 treated supra-coronary aortic banding rats (SAB) rats but not in siControl treated SAB rats. There is no significant difference in PKM2 expression in the J) small pulmonary arteries.

Supplementary Figures

Supplementary Figure 1. Hemodynamic studies showing A) cardiac output (CO) and B) pulmonary vascular resistance (PVR) in the shikonin and silencing pyruvate kinase muscle isoform 2 (siPKM2) treated supra-coronary aortic banding (SAB) rats vs. DMSO and silencing control (siControl) treated SAB rats.

Supplementary Figure 2. The effect of shikonin administration on rat weight. Shikonin administration 2mg/kg IP daily caused a slight but marked decrease in weight that stabilized after one week.

Supplementary Figure 3. The effect of shikonin on left ventricle (LV) weight, right ventricle (RV) weight, and proximal banding blood pressure. A) There is no difference in LV weight in supra-coronary aortic banding (SAB) rat treated with shikonin vs. DMSO. B) There is significant reduction in RV weight in SAB rat treated with shikonin vs. DMSO. C) There is a trend towards Fulton Index reduction in shikonin treated SAB rats vs. DMSO control. D) There is no change in LV + septum to body weight ratio. E) There is a significant reduction in RV to body weight ratio SAB shikonin rats vs. SAB DMSO. F & G) There is no significant change in proximal systolic and diastolic blood pressure (pSBP & pDBP) caused by the band in shikonin or DMSO treated SAB rat.

Supplementary Figure 4. Design and validation of silencing PKM2 messenger RNA. PKM2 expression is much higher than PKM1 in monocrotaline rat pulmonary artery smooth muscle cells. However, siPKM2 is able to knock down the expression of both PKM2 and PKM1.

Supplementary Figure 5. Immunoblot showing reduction of PKM2/PKM1 ratio in shikonin treated SAB rats compared to SAB rats treated with DMSO.
Western blot of left ventricle (LV) showing upregulation of PKM2 and down-regulation of PKM1 in the SAB-DMSO rats, and treatment with shikonin (2 mg IP daily for 2-week) in SAB rat reduced the expression of PKM2/PKM1 ratio.

Supplementary Figure 6. Additional Western blot images showing reduction of PKM2/PKM1 ratio in shikonin or sPKM2 treated SAB rats compared to SAB rats treated with DMSO and siControl. These data were included in summary plots of figure 6.

Supplementary Figure 7. Representative images showing the hand-drawn tracing of the pulmonary artery media used to measure PKM1 and PKM2 expression in the small pulmonary arteries.

Acknowledgement

SLA is funded by a Foundation grant from the Canadian Institutes for Health Research (CIHR) and grants from the National Institutes of Health (R01-HL071115, 1RC1HL099462), Canada Foundation for Innovation (229252 and 33012), a Tier 1 Canada Research Chair in Mitochondrial Dynamics and Translational Medicine (950-229252), and a grant from the William J Henderson Foundation. The research is supported by the Queen's Cardiopulmonary Unit.

Figure 1. Experimental design

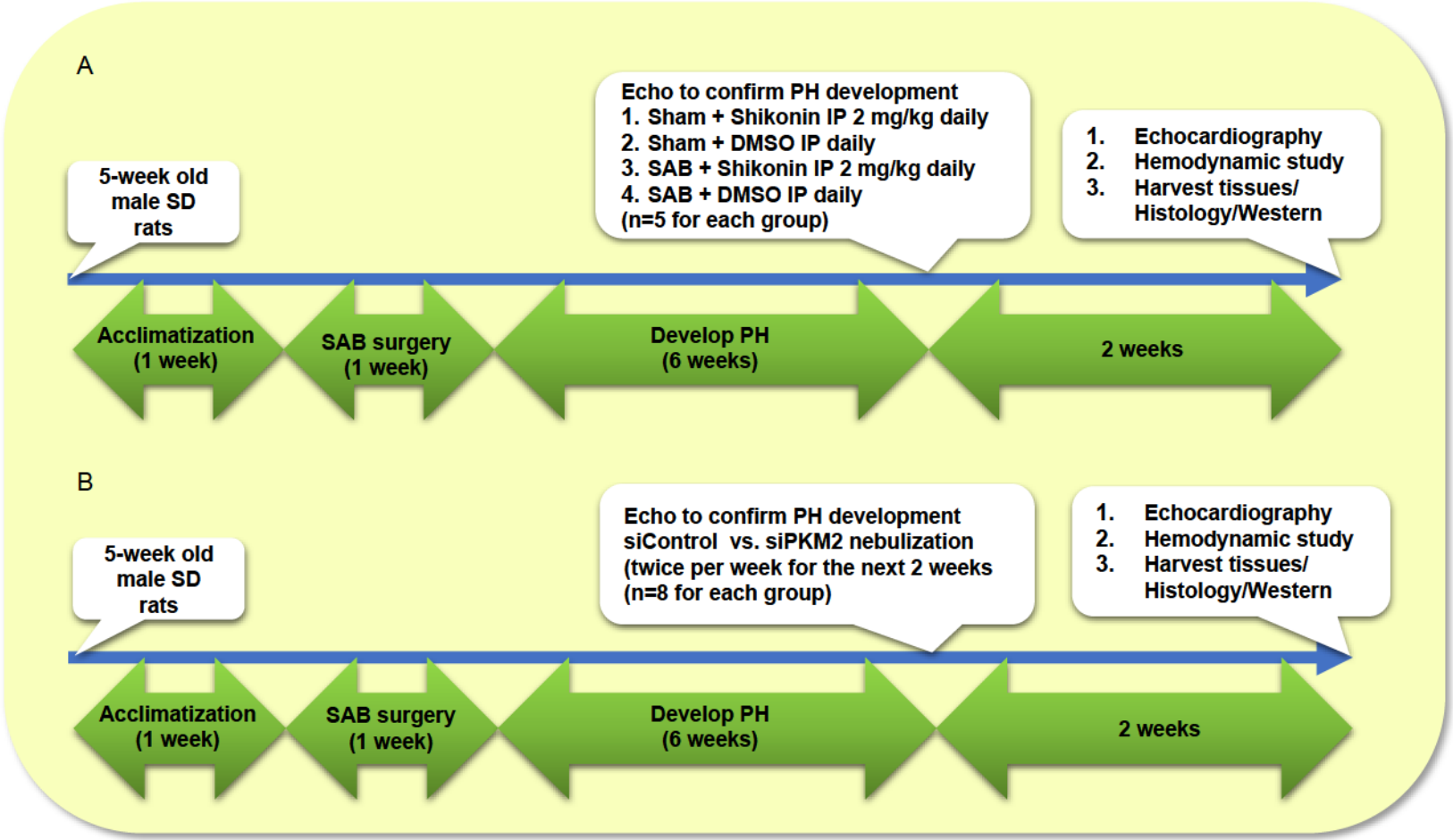

Figure 2. ECHO pre- and post- shikonin and siPKM2 treatment

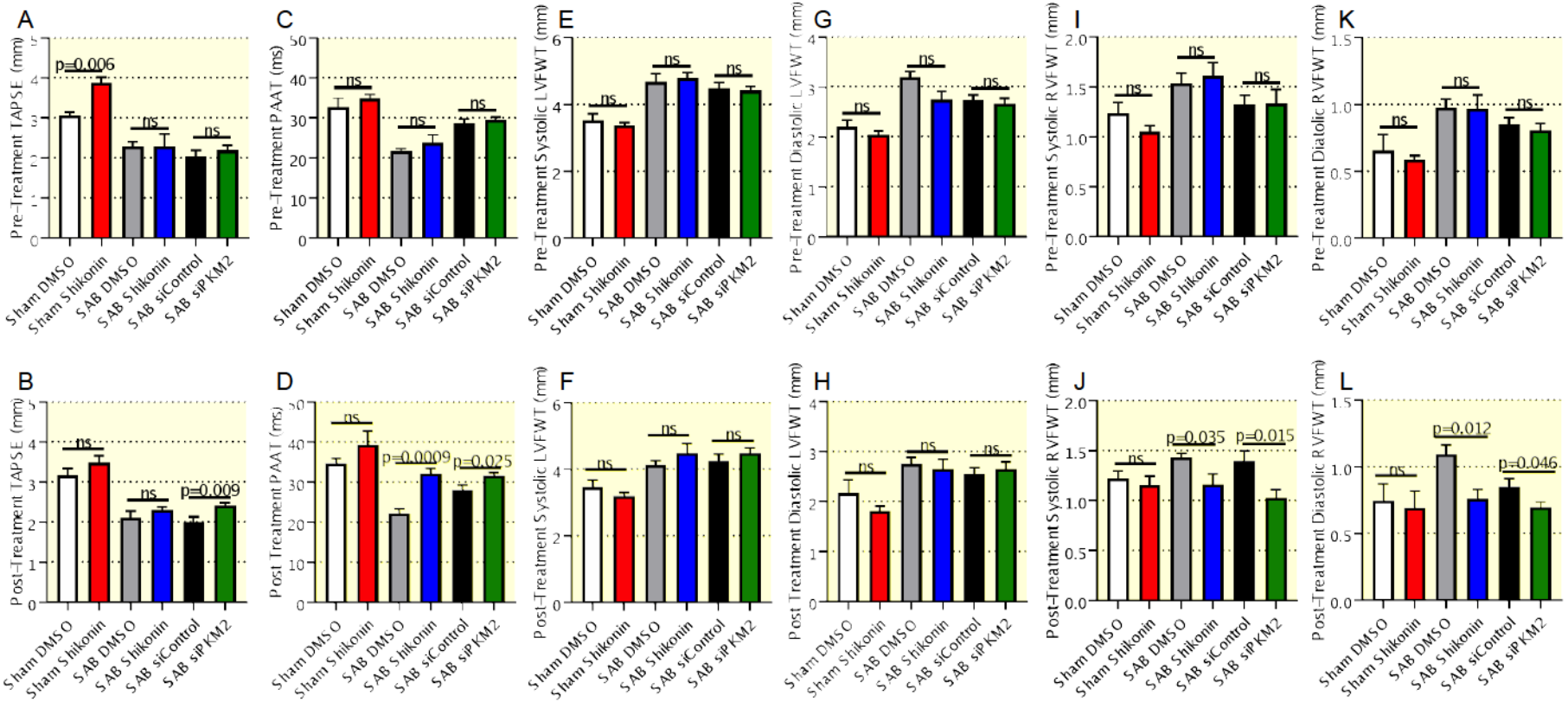

Figure 3. Hemodynamics post shikonin and siPKM2 treatment.

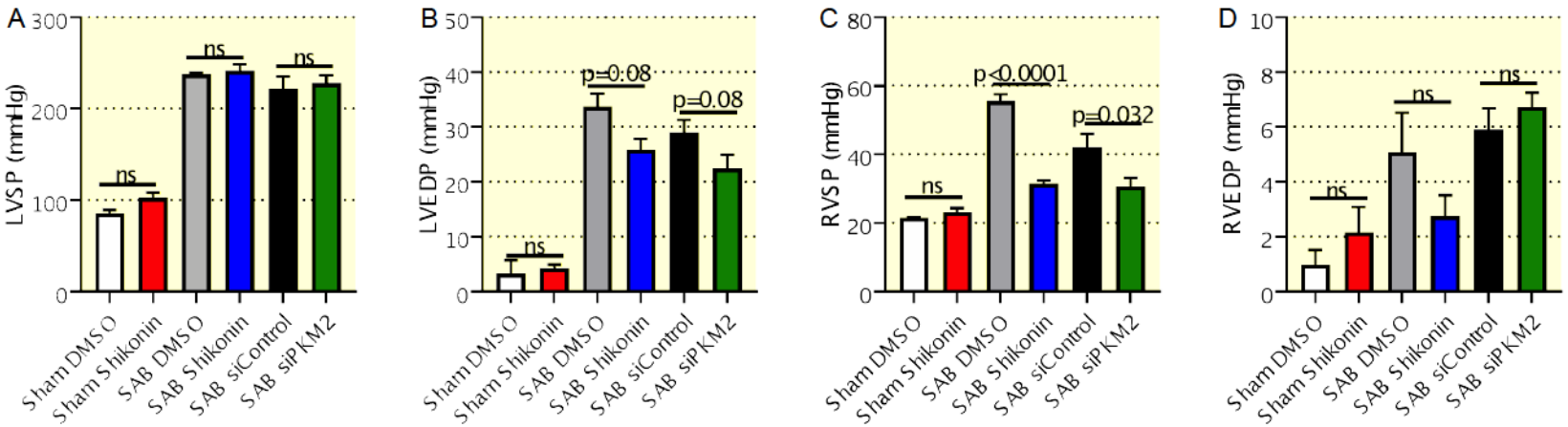

Figure 4. RV histology and RV myocyte size

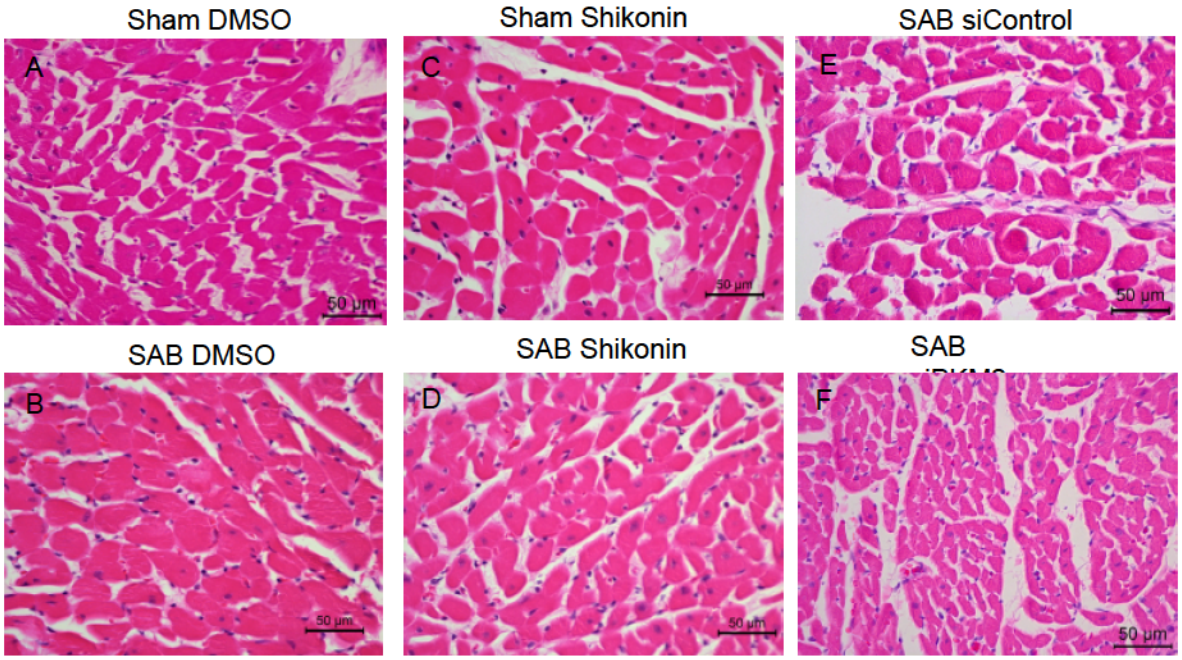

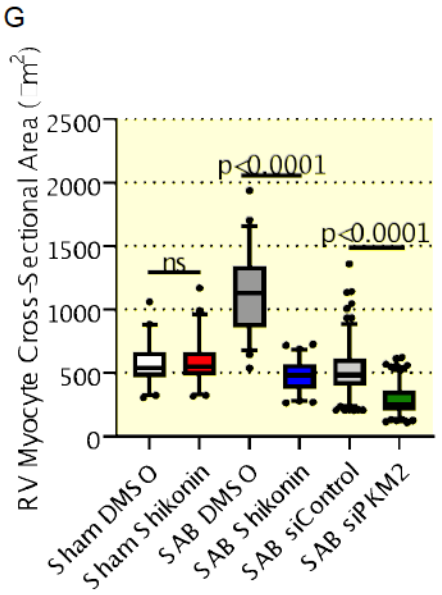

Figure 5. Lung histology and lung myocyte size

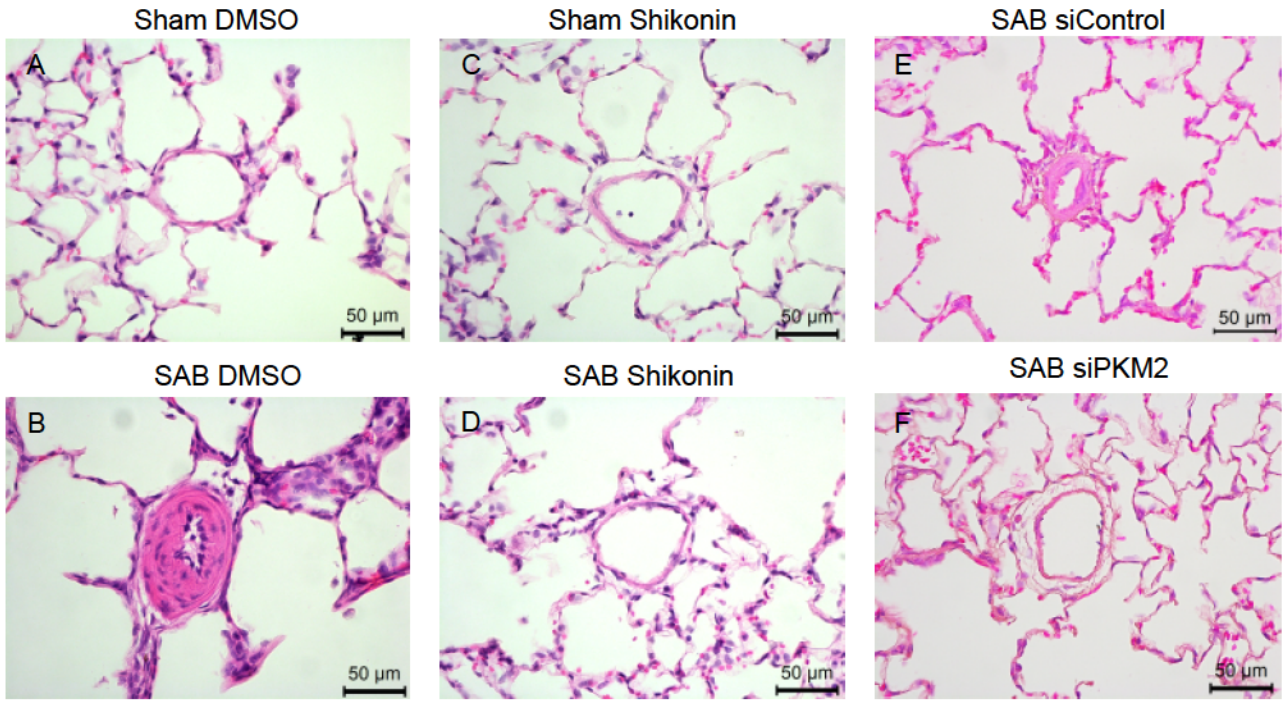

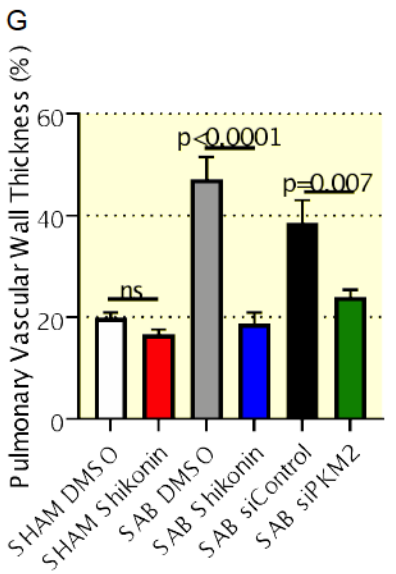

Figure 6. RV Western Representative blot

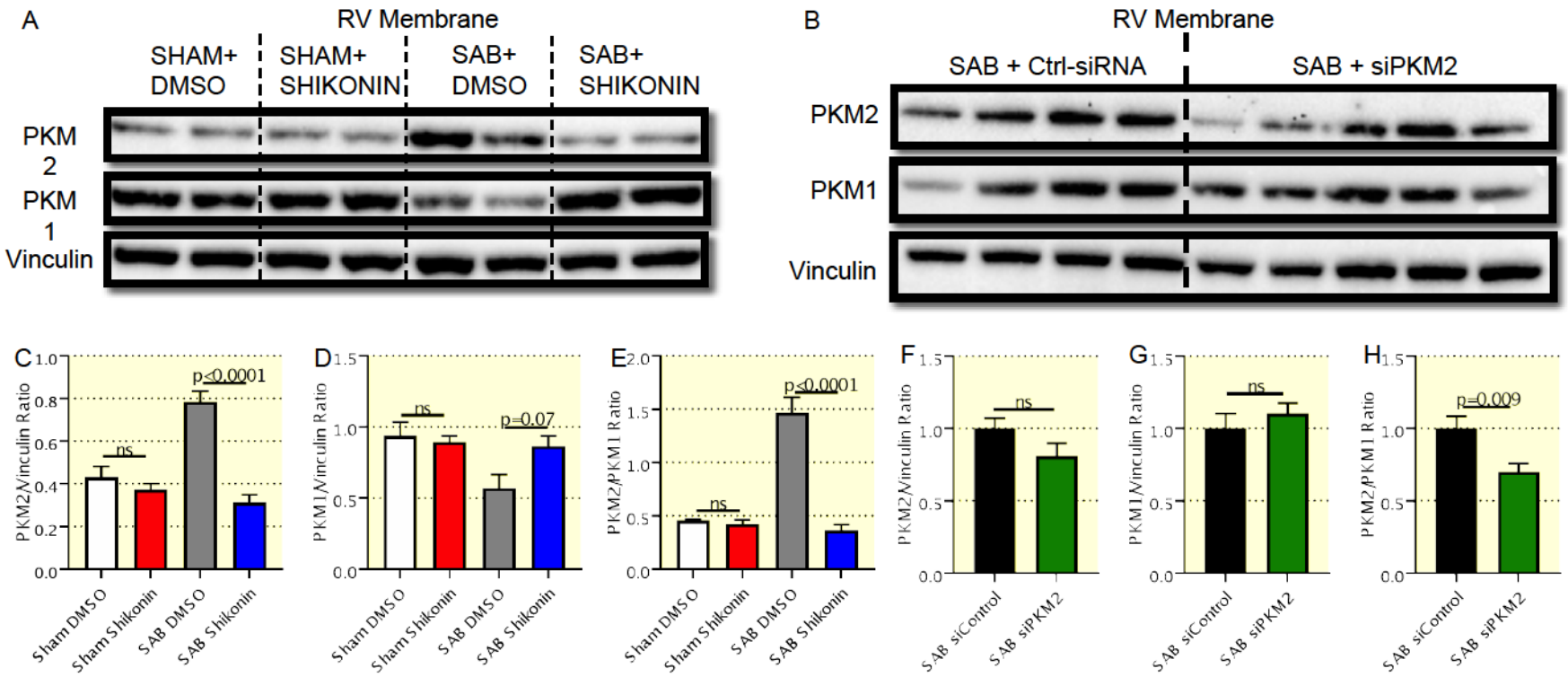

Figure 7. PKM1 expression in whole lung and small pulmonary artery.

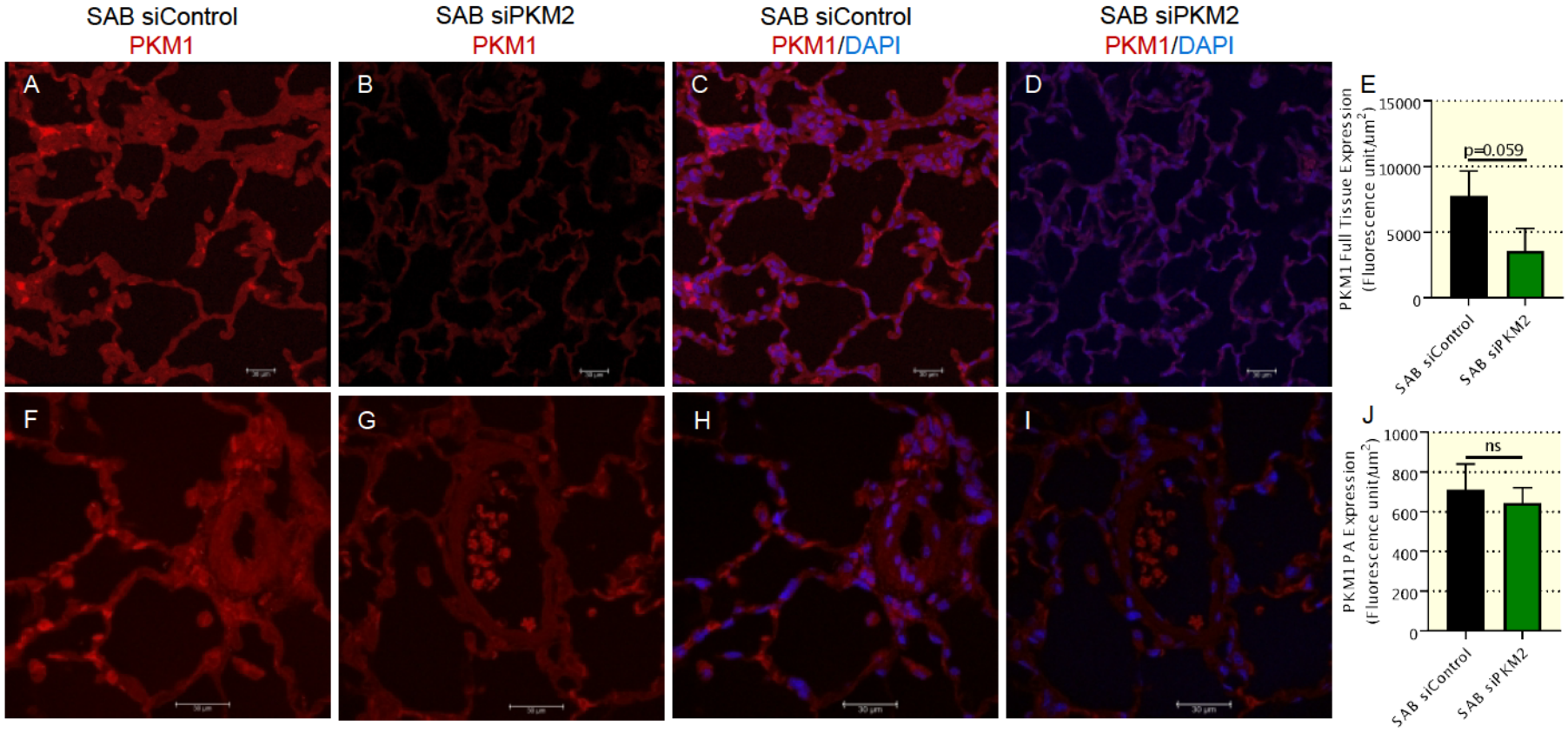

Figure 8. PKM2 expression in whole lung and small pulmonary artery.

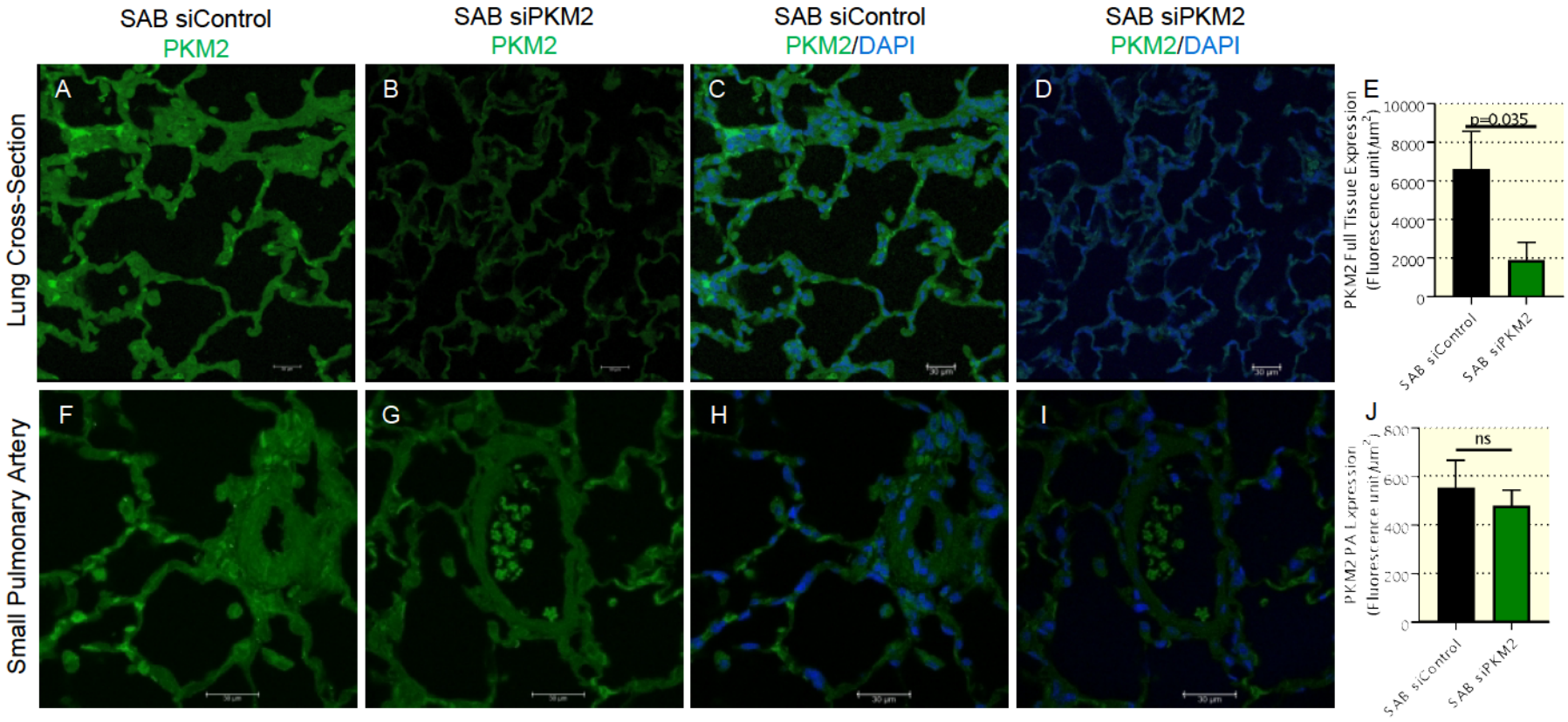

Supplementary Figures

Supplementary Figure 1. hemodynamic data

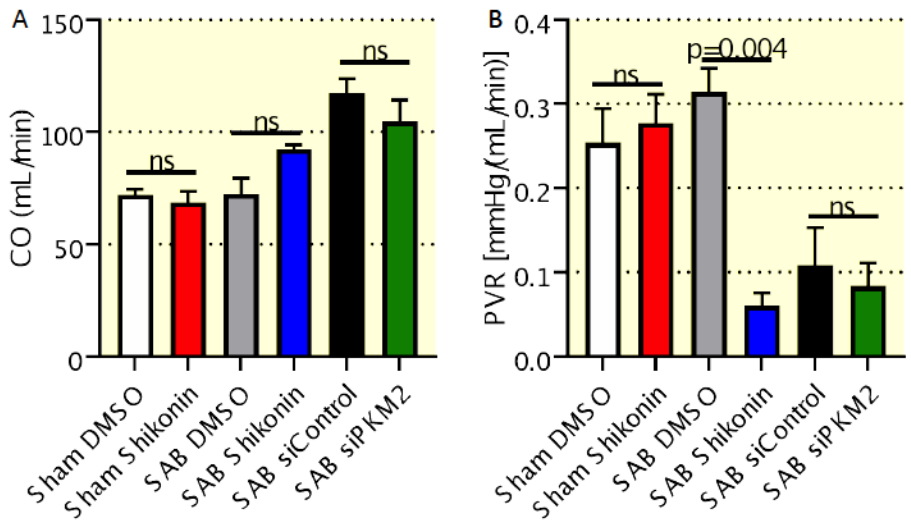

Supplementary Figure 2. Effect of shikonin on rat body weight.

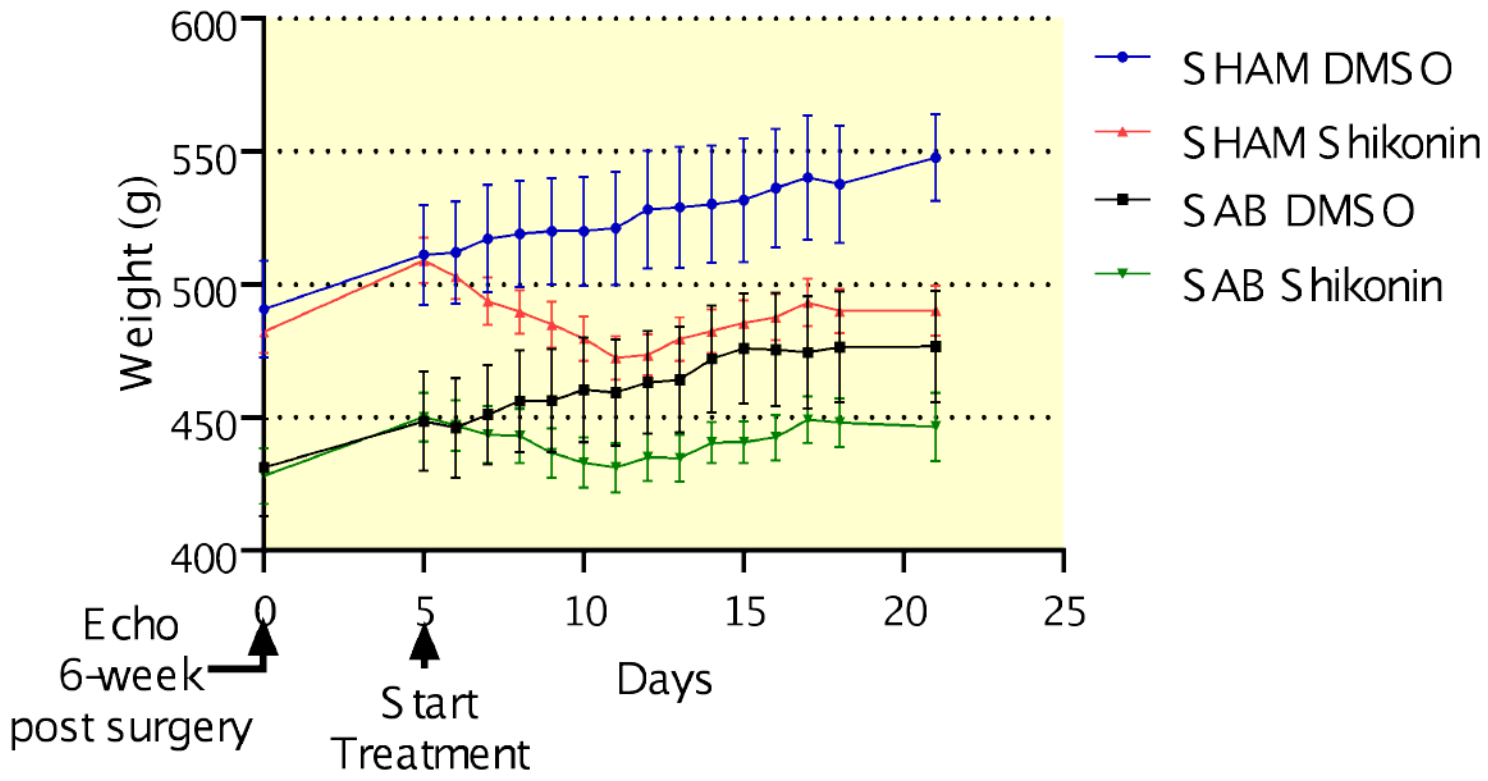

Supplementary Figure 3. Shikonin caused marked reduction in RV to body weight ratio compared to DMSO treated rats.

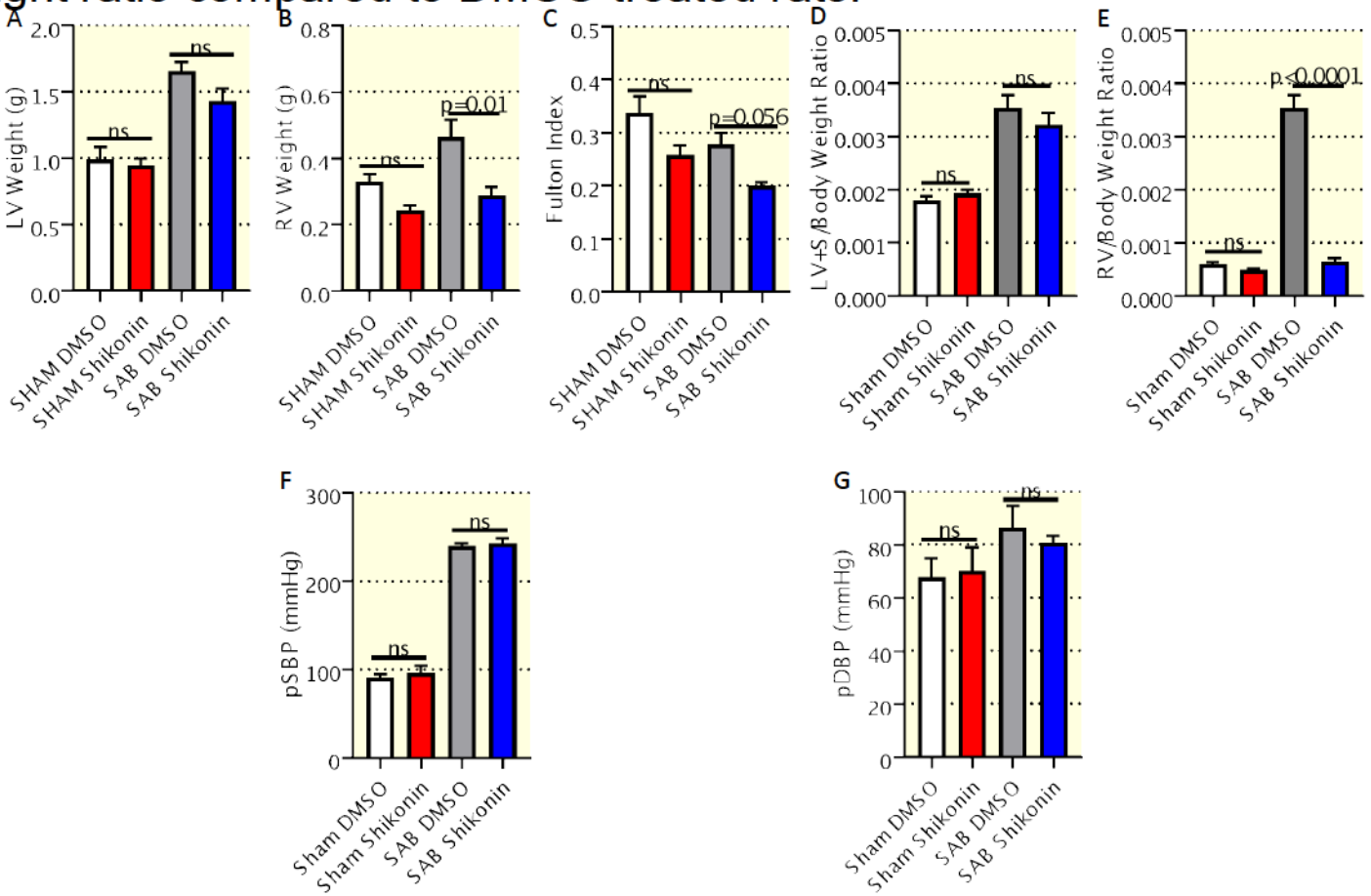

Supplementary Figure 4. MCT rat RV Fibroblast transfected with siPKM2s (1, 3, 5, and 7) Amplified with rat PKM2 primers

- **siPKM2-1: 5' GGG CUG AGG ACG UUG AUC U UU 3'**
- **siPKM2-2: 5' GUG UGA ACU UGG CCA UGA A UU 3'**
- **siPKM2-3: 5' CGU UGA UCU UCG UGU GAA C UU 3'**
- **siPKM2-7: 5' UGA ACU UGG CCA UGA AUG U UU 3'**

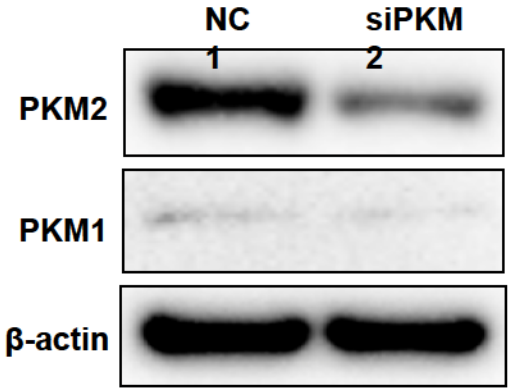

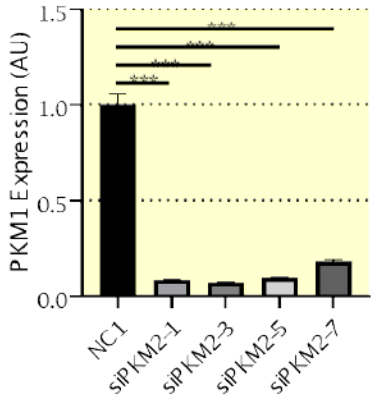

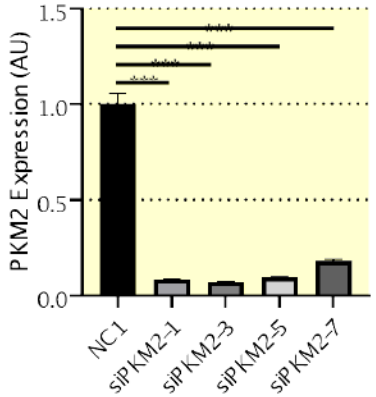

Supplementary Figure 5. LV Western blot

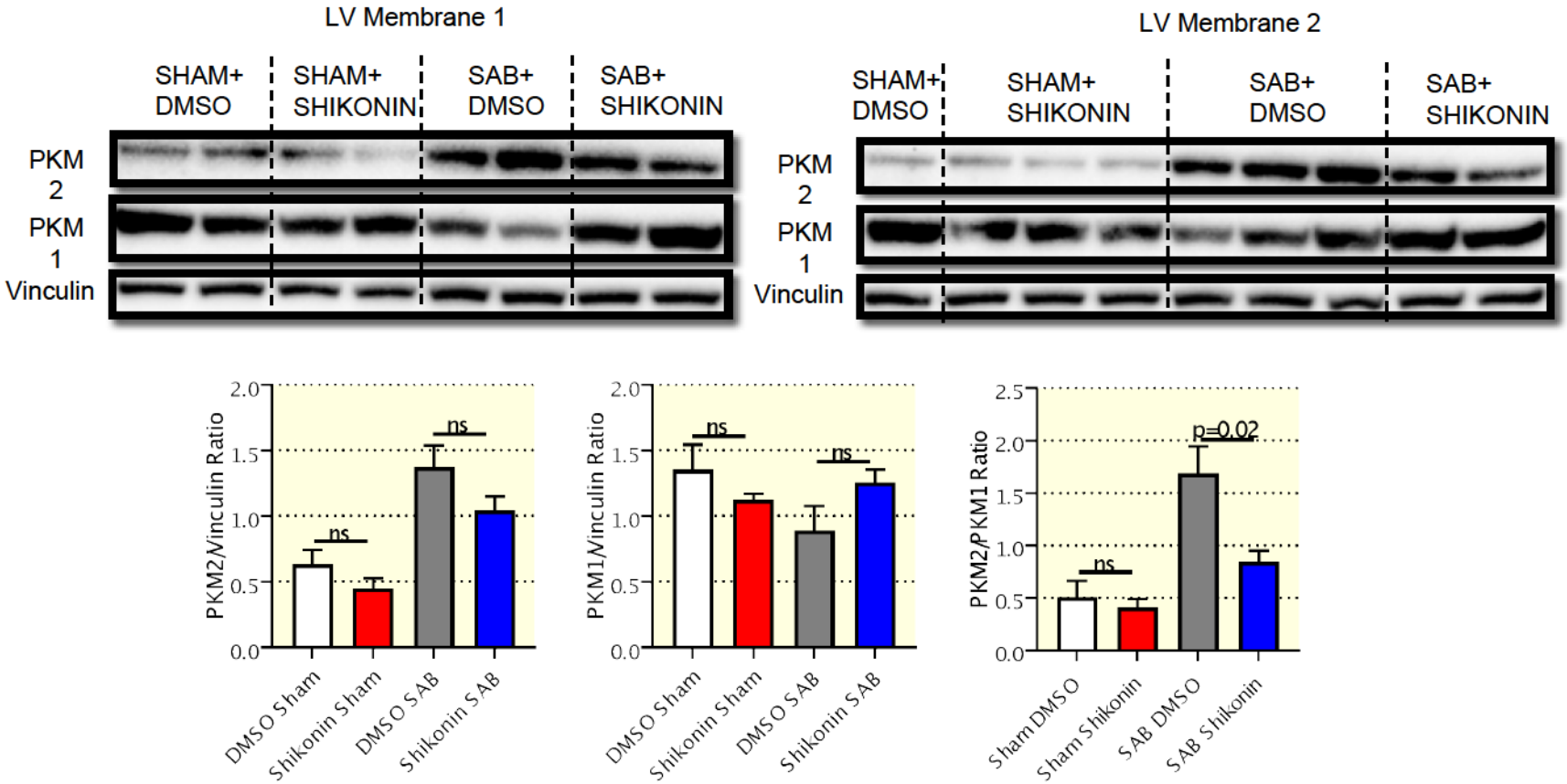

Supplementary Figure 6. Additional RV Western blot

Supplementary Figure 7. Representative images showing the hand-drawn tracing of the pulmonary artery media.